Structural Engineering and Mechanics, *Vol. 60, No. 6 (2016) 1001-1019*
DOI: http://dx.doi.org/10.12989/sem.2016.60.6.1001

Behavior of steel and concrete composite beams with a newly puzzle shape of crestbond rib shear connector: an experimental study

Van Phuoc Nhan Le[1a], Duc Vinh Bui[1b], Thi Hai Vinh Chu[2c], In-Tae Kim[3d], Jin-Hee Ahn[4e] and Duy Kien Dao[*3]

[1]Department of Civil Engineering, Ho Chi Minh City University of Technology, 268 Ly Thuong Kiet Street, Ward 14, District 10, Ho Chi Minh City, Vietnam
[2]Faculty of Civil Engineering, MienTrung University of Civil Engineering ,24 Nguyen Du Street, Ward 7, Tuy Hoa City, Phu Yen,Vietnam
[3]Department of Civil Engineering, Pusan National University, 30 Jangjoen-dong, Geumjeong-gu, Busan 609-735, Korea
[4]Department of Civil Engineering, Gyeongnam National University of Science and Technology, Korea 30 Donghin-Ro, Jinju, Gyeongnam 660-758, South Korea

(Received June 21, 2016, Revised July 28, 2016, Accepted October 5, 2016)

Abstract. The connector is the most important part of a composite beam and promotes a composite action between a steel beam and concrete slab. This paper presents the experiment results for three large-scale beams with a newly puzzle shape of crestbond. The behavior of this connector in a composite beam was investigated, and the results were correlated with those obtained from push-out-test specimens. Four-point-bending load testing was carried out on steel-concrete composite beam models to consider the effects of the concrete strength, number of transverse rebars in the crestbond, and width of the concrete slab. Then, the deflection, ultimate load, and strains of the concrete, steel beam, and crestbond; the relative slip between the steel beam and the concrete slab at the end of the beams; and the failure mechanism were observed. The results showed that the general behavior of a steel-concrete composite beam using the newly puzzle shape of crestbond shear connectors was similar to that of a steel-concrete composite beam using conventional shear connectors. These newly puzzle shape of crestbond shear connectors can be used as shear connectors, and should be considered for application in composite bridges, which have a large number of steel beams.

Keywords: crestbond rib shear connector; concrete-steel composite beam; composite behavior; loading test; shear resistance formula

---

*Corresponding author, Ph.D. Candidate, E-mail: kiendaoduy@gmail.com
[a]Ph.D., E-mail: lvpnhan@hcmut.edu.vn
[b]Ph.D., E-mail: vinhbd@hcmut.edu.vn
[c]Master, E-mail: chuthihaivinh@muce.edu.vn
[d]Professor, E-mail: itkim@pusan.ac.kr
[e]Assistant Professor, E-mail: jhahn@gntech.ac.kr

http://www.techno-press.org/?journal=sem&subpage=8 ISSN: 1225-4568 (Print), 1598-6217 (Online)

1. Introduction

A perfobond shear connector is a typical rigid shear connector. It consists of a flat steel pale with holes, and its shear resistance strength is provided by the concrete end bearing, concrete dowel resistance of the holes, and rebar penetrating the holes. The perfobond rib shear connector was first developed by Leonhardt, Andrä *et al.*. (1987). After this, many researchers examined its composite behavior and shear strength for applications to composite or mixed structures to take advantage of its higher shear resistance strength, easy fabrication, etc. (Ahn, Lee *et al.* 2010, Mohammad 2011, Xue, Liu *et al.* 2012, Shim, Lee *et al.* 2011, Shariati, Ramli *et al.* 2011). Modified perfobond rib connectors were also suggested by several researchers (Kim, Lee *et al.* 2010, Kim, Ahn *et al.* 2011). Then, the composite behaviors and shear strengths of a T-shaped perfobond rib, Y-shaped perfobond rib (Kim, Choi *et al.* 2013, Kim, Choi *et al.* 2014a, Kim, Park *et al.* 2015, Kim, Heo *et al.* 2014b), Y-shaped perfobond with open holes (Kim, Kim *et al.* 2016), etc. were examined.

Among the newly modified perfobond rib shear connectors, a perfobond with open holes is called a crestbond rib because of its appearance. This crestbond rib (perfobond with open holes) shear connector allows the easy installation of rebar because of its open rib holes. In addition, it has a higher shear resistance strength than a typical perfobond rib. Fig. 1 shows the currently suggested crestbond rib shear connector. Research has been conducted to examine its composite behaviors and shear strength. Bui (2010) carried out a detailed study of structural composite beams with typical perfobond ribs and crestbond ribs using ultra-high-performance concrete (UHPC) with a compressive strength of 140-180 MPa. The existence of open holes can create an advantage in placing reinforcing bars though the holes. The open holes of crestbond rib shear connectors were designed to be able to obtain two crestbond ribs when cutting a steel rib (PreCo-Beam 2006, Preco+ 2011). It is welded along the length of a steel beam at the interface of the concrete slab and top flange of the steel beam. However, there have been relatively few studies on crestbond rib shear connectors compared to those on perfobond ribs, and various parameters were not considered (Chromiak and Studnicka 2006). Lorenc, Kubica *et al.* (2010), Lorenc, Kożuch *et al.* (2014) Part I, Lorenc, Kożuch *et al.* (2014) Part II proposed a new type of crestbond where the steel connector constitutes an integral part of the steel part of the composite beam, which is subjected, apart from the local longitudinal shear acting between the steel and concrete, to the global effects of bending and axial loading. The stress criteria describing a composite dowel's behavior must be established and involve much more than the pure load-bearing capacity criteria used at present. Test procedures combining the concept of the load-bearing capacity of the concrete part of the connector and the elasticity of its steel part lead to the efficient design of composite structures. The opened holes made the assembly of the concrete slab steel reinforcement easier. Other opening shapes for perforated ribs have been developed by Rovnak, Duricova *et al.* (2000), as shown in Fig. 1. A crestbond with a modified rib shape was proposed because the shape of the open holes in the rib plate can be modified or revised depending on the fabrication process, etc.

For this reason, a newly puzzle shape of crestbond rib connector with a "ʊ" shape was proposed by Chu, Bui *et al.* (2016) as shown in Fig. 2. To reduce the stress concentration on steel dowel, the steel - dowel and dowel - root were redesigned more circular, and the dowel - core is lager. Its shear resistance strengths and composite behaviors were examined in a push-out test, six push-out test specimens were fabricated, and five main parameters were considered in the push-out specimens to evaluate the effects of shear resistance parameters such as the dimensions of the

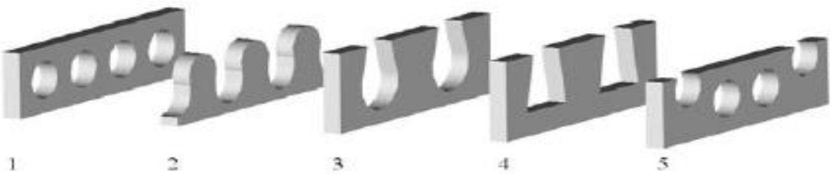

Fig. 1 Suggested open-hole types of rib shear connectors: 1-Leonhardt, 2-Rovnak, 3-Kraus, 4-Kunzel, and 5-Andrä (Rovnak, Duricova *et al.* 2000, Kraus and Würzer 1997).

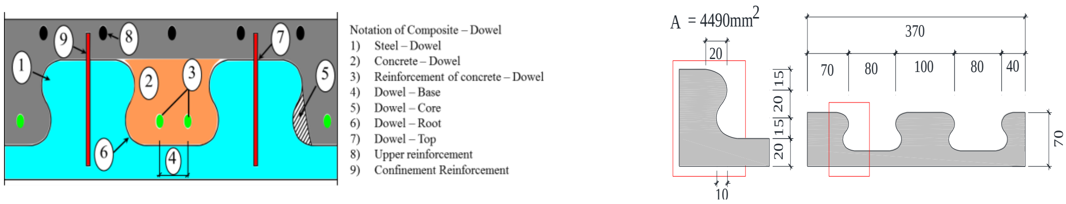

(a) Components of a Composite Dowel concept (PreCo-Beam 2006, Preco+ 2011)

(b) The Dimensions of newly modified crestbond rib shear connector

Fig. 2 The newly revised crestbond shear connector: concept (a) and dimensions (b) (Chu, Bui *et al.* 2016).

crestbond rib, transverse rebars in the crestbond dowel, concrete strength, rebar strength, and dowel action on the shear strength, and a design equation was proposed based on the test results. However, its applicability to a composite beam as a shear connector was not examined. In this study, therefore, static loading tests were conducted on a composite beam with a newly puzzle shape of crestbond rib. Three full-size steel-concrete composite beams with newly puzzle shape of crestbond ribs were fabricated to compare the composite behaviors in relation to the transverse reinforcement and concrete compressive strength. Based on loading tests, their structural behaviors such as their loading capacities, deflections, relative slips, crestbond rib strains, and failure mechanisms were quantitatively examined.

2. Loading test conditions

2.1 Test specimens

To examine the applicability and composite behaviors of the newly puzzle shape of crestbond shear connector in composite beams under loading, three full-size composite beams were prepared (B1, B2, and B3). Each composite beam had a 4000 mm of length and a concrete slab that was 120 mm thick and 600 mm wide. Two longitudinal rebars with a diameter of 12 mm were installed in this concrete slab. An H beam with a height of 244 mm and flange width of 175 mm was used. For the shear connector, a continuous crestbond rib shear connector with a height of 70 mm and a thickness of 8 mm was attached to the top flange of the steel H beam, as shown in Fig. 4.

For the transverse rebars in the crestbond holes, composite beam specimens B1 and B3 used two transverse rebars passing through each of the crestbond holes, whereas composite beam specimen B2 used a single transverse rebar passing through every other hole, as shown in Fig. 5. A 12-mm rebar was used as the transverse rebar for the crestbond rib holes. The compressive strength of the concrete slab was considered as the main parameter. The concrete material properties of composite beam specimens B2 and B3 were changed to 39.9 MPa and 50.4 MPa, respectively. When designing the composite beam specimens, their plastic moment resistances

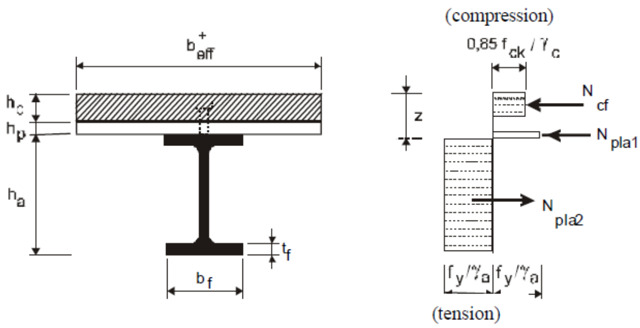

Fig. 3 Plastic distribution of normal stresses: example of plastic neutral axis in steel flange (C.-E.C.f. Standardisation)

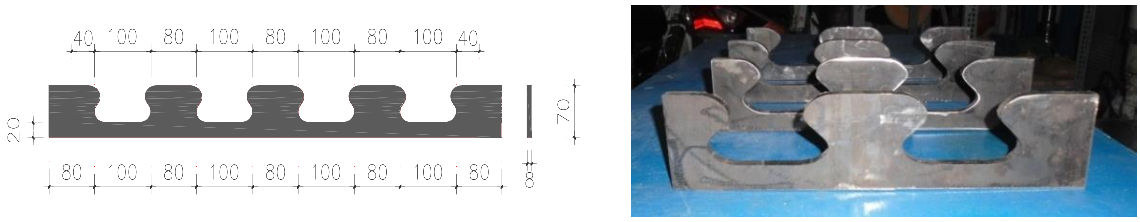

Fig. 4 Dimensions of crestbond connector used

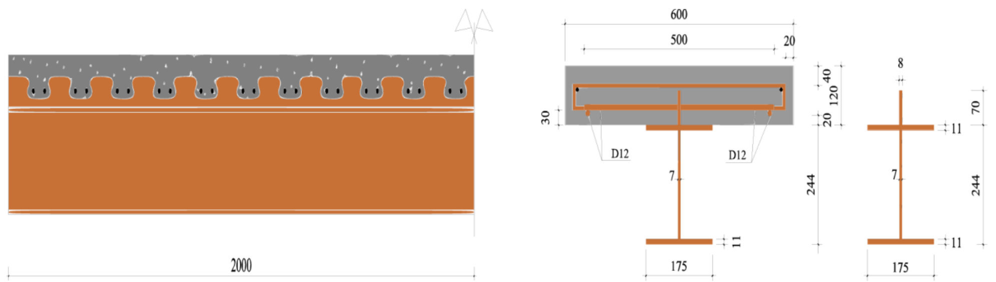

(a) Composite beam specimen B1

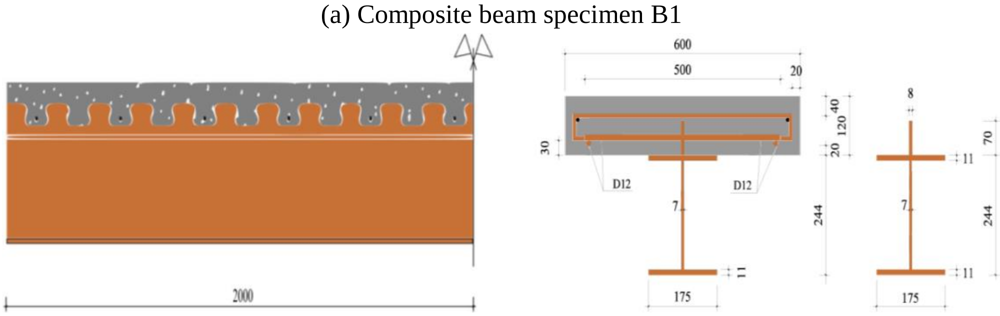

(b) Composite beam specimen B2

Fig. 5 Dimensions of composite beam specimen

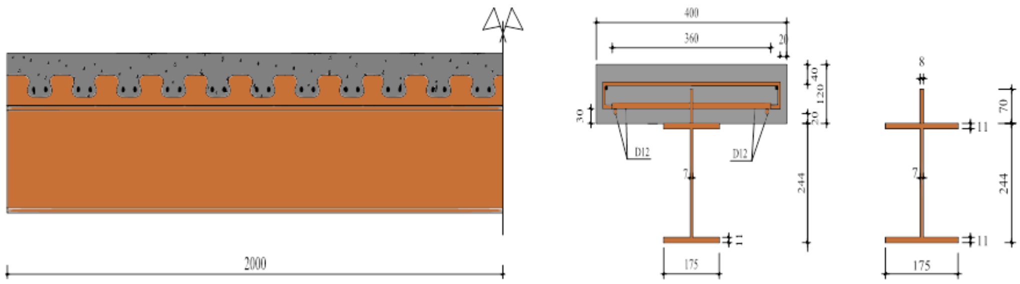

(c) Composite beam specimen B3

Fig. 5 Continued

Table 1 Composite beam specimens

	Concrete slab			Steel beam	No. of transverse reinforcement	Note
	Grade	Compressive strength f_c	Section (H×W)			
		MPa	mm			
B1	C30	39.9	120×600	H244×175	2	All holes
B2	C30	39.9	120×600	H244×175	1	Alternate holes
B3	C40	50.4	120×400	H244×175	2	All holes

along the neutral axis located at the exposure surface between the steel beam and concrete slab were determined using Eurocode-4 (2004), as shown in Fig. 3, and the value of the plastic moment was calculated following Eq. (1). Thus, the plastic moments of B1 and B2 were determined to be 310 kN.m, and that of B3 was determined to be 324 kN.m.

$$M^{+}_{pl.Rd} = N_{pla}(0{,}5h_a + 0{,}5h_c + h_p) - 0{,}5(N_{pla} - N_{cf})(z + h_p) \tag{1}$$

where $M^{+}_{pl.Rd}$ is the plastic moment; N_{pla} and N_{cf} are the plastic axial resistances of the steel beam (in tension) and concrete slab (in compression), respectively; z is the depth of the plastic neutral axis; and h_a, h_c, and h_p are the height of the steel beam, height of the compressive area, and depth of the profiles, respectively.

The shear strength of the newly puzzle shape of crestbond rib shear connector was determined by the push-out test results and suggested design equation (Chu, Bui *et al*. 2016), and the degree of the shear connection of the composite beam specimen was determined to be a full shear connection. The sectional and material characteristics of each composite beam specimen are summarized in Table 1.

2.2 Material properties

To examine the material properties of the concrete, concrete cube and cylinder specimens were fabricated at the same time as the concrete slab for each beam was cast. The ratios 0.52 and 0.34 of Water/ Cement (W/C) were applied to fabricate the concrete B25 and B40, respectively. These specimens were cured under the same conditions as the composite beam specimens. The concrete cube specimens were used to measure the compressive strength and strain of the concrete, while the concrete cylinder specimens were used to measure the Poisson's ratio and elastic modulus of the concrete. These material properties were measured on the same day that the composite beam

Table 2 Material properties of composite beam specimen

Concrete				Steel beam and crestbond rib			
Number of test specimen	Compressivestrength (f_c)	Young Modulus (E_c)	Flexural strength (f_{ct})	Number of test specimen	Yield Strength (f_y)	Ultimate strength (f_u)	Young modulus
	MPa	MPa	MPa		MPa	MPa	MPa
B25-1	35.9	29×10^3	3.42	ST-1	253	395	200×10^3
B25-2	35.5	29×10^3	3.34	ST-2	255	390	201×10^3
B25-3	35.1	29×10^3	3.37	ST-3	248	386	201×10^3
B40-1	50.4	33×10^3	3.63				
B40-2	50.9	33×10^3	3.60				
B40-3	50.0	33×10^3	3.52				

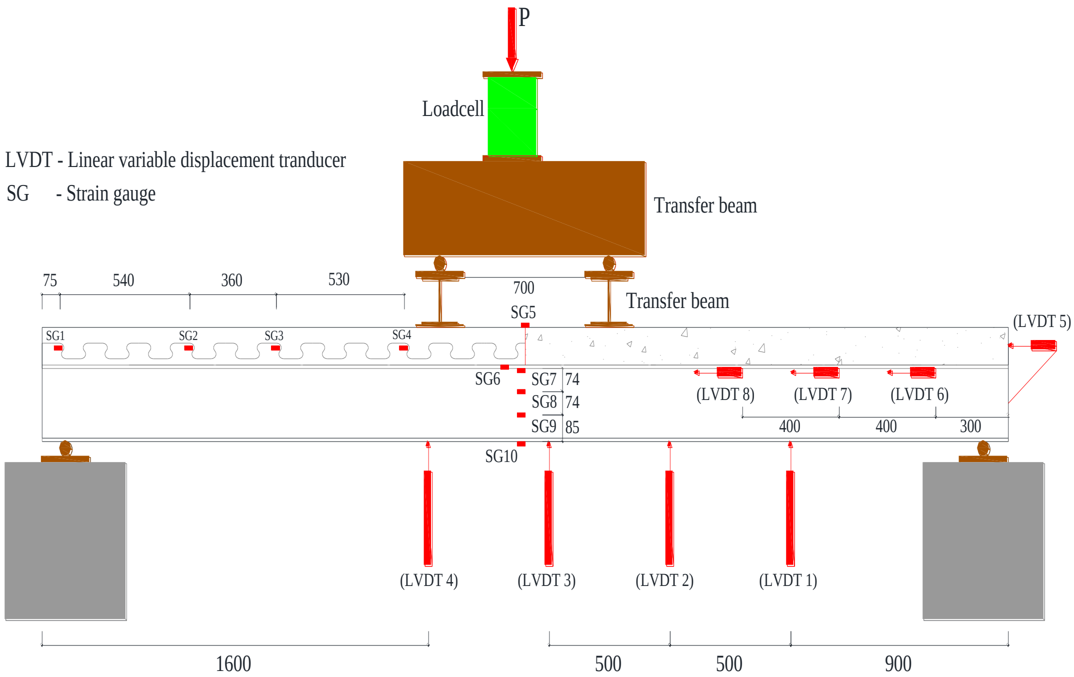

Fig. 6 Test schematic and arrangement of instruments.

specimens were tested. The material properties of the concrete, steel beam, and crestbond rib are presented in Table 2. The yield strength and ultimate strength of the transverse and longitudinal rebars were 250 MPa and 390 MPa, respectively.

2.3 Test setup

A hydraulic jack was used to apply a load to the composite beam with the newly puzzle shape of crestbond rib. To apply a four-point-bending moment to the composite beam specimen, two lateral steel transfer beams were placed at distances of 350 mm from the mid-span. To measure the relative slip at the composite interface, deflection, and strain distributions of the composite beam, strain gauges and linear variable displacement transducers (LVDTs) were installed as shown in Fig. 6. Accordingly, these are the important positions to determine the failure of crestbond rib, concrete slab, and steel beam that maximum stress is occurred.

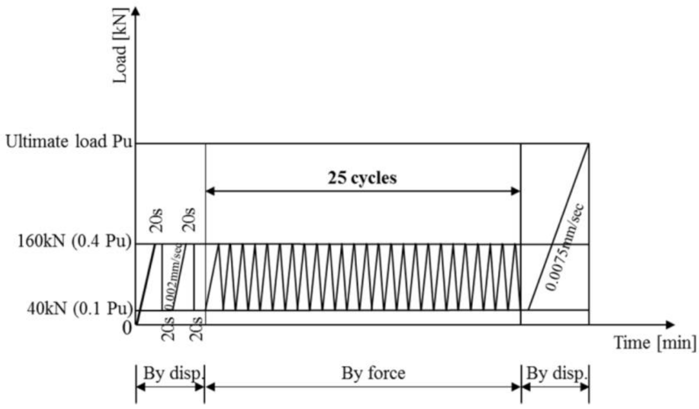

Fig. 7 Loading increment schedule

(a) Test setup

(b) Deflection measurement

(c) Relative slip measurement

(d) Strain measurement of the concrete slab

Fig. 8 Test setup and instrumentation

(e) Strain measurement of the crestbond connector

(f) Strain measurement of the steel beam

Fig. 8 Continued

Table 3 Test results

Beam	P_u (kN)	Deflection (mm)	Relative slip (mm)	Plastic moment		Failure mode
				Test (kN.m)	Design (kN.m)	
B1	407.6	49.95	1.16	315.6	310	Plastic failure happened at steel girder and concrete slab
B2	394.9	65.11	0.94	306.1	310	Plastic failure happened at steel girder and concrete slab
B3	418.8	40.03	0.341	324.6	324	Plastic failure happened at steel girder and concrete slab

The loading was varied according to the schedule shown in Fig. 7. First, the composite beam specimens were loaded to 40% of the predicted failure load and then unloaded. Then, this load level was repeated 25 times to eliminate friction between the concrete slab and the steel beam. Finally, loading tests were conducted at loads increasing toward the ultimate load, P_{max}. These loading tests were terminated after decreasing the load back to 90% of P_{max}. Fig. 8 shows the test setup and instrumentation.

3. Results and discussion

3.1 Summary of test results

The results of four-point loading tests were compared to assess the behaviors of composite beams with the newly puzzle shape of crestbond in relation to the number of transverse rebars and concrete strength. Table 3 summarizes the loading test results of the composite beam specimens, including the deflections, relative slips at the composite interface, and strains of the concrete slab, steel beam, and crestbond rib. Their failure modes included failures of the concrete slab and steel beam. No failure of the crestbond rib was found.

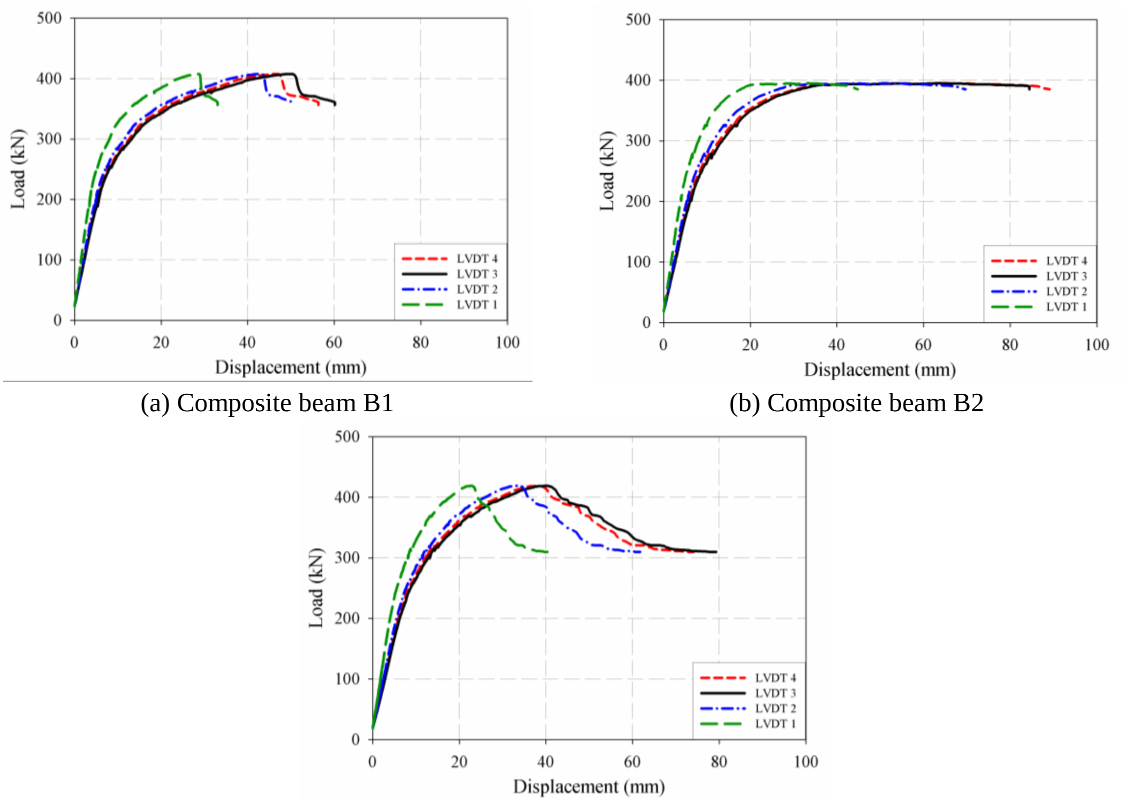

(a) Composite beam B1

(b) Composite beam B2

(c) Composite beam B3

Fig. 9 Load–displacement relationships

3.2 Load–displacement relationships and load–deflection relationships

To examine the structural behaviors of composite beam specimens with the newly puzzle shape of crestbond, their load–displacement and load-deflection relationships were compared using four LVDTs placed at locations that were 0.8 m, 1.3 m, 1.9 m, and 2.25 m from the right end of the composite beam, named LVDT1 to LVDT4, respectively. Figure 9 shows their load–displacement curves at each measured position. As shown in Fig. 9 and Table 3, composite beam specimen B1 had a higher ultimate load than specimen B2, and composite beam specimen B3 had a higher ultimate load than specimen B1. This can naturally be explained by the fact that the transverse 000000rebar in the crestbond hole and the concrete strength affect the load-carrying capacity of a composite beam with the newly puzzle shape of crestbond rib. However, specimen B2 with a single transverse rebar installed in a crestbond rib hole showed higher ductile behaviors in the push-out test results (Chu, Bui *et al.* 2016). The transverse rebar in the crestbond rib hole can be considered related to the structural characteristics. Fig. 10 shows the deflection of the composite beam specimens in relation to the load level. The deflection was significantly increased at 80% of the ultimate load (P_{max}) because a structural transition from an elastic to a plastic behavior began. In particular, the deflection of composite beam specimen B2 was relatively more sharply increased because of its ductile behaviors. Fig. 11 compares the curves of the load vs. deflection at the mid-

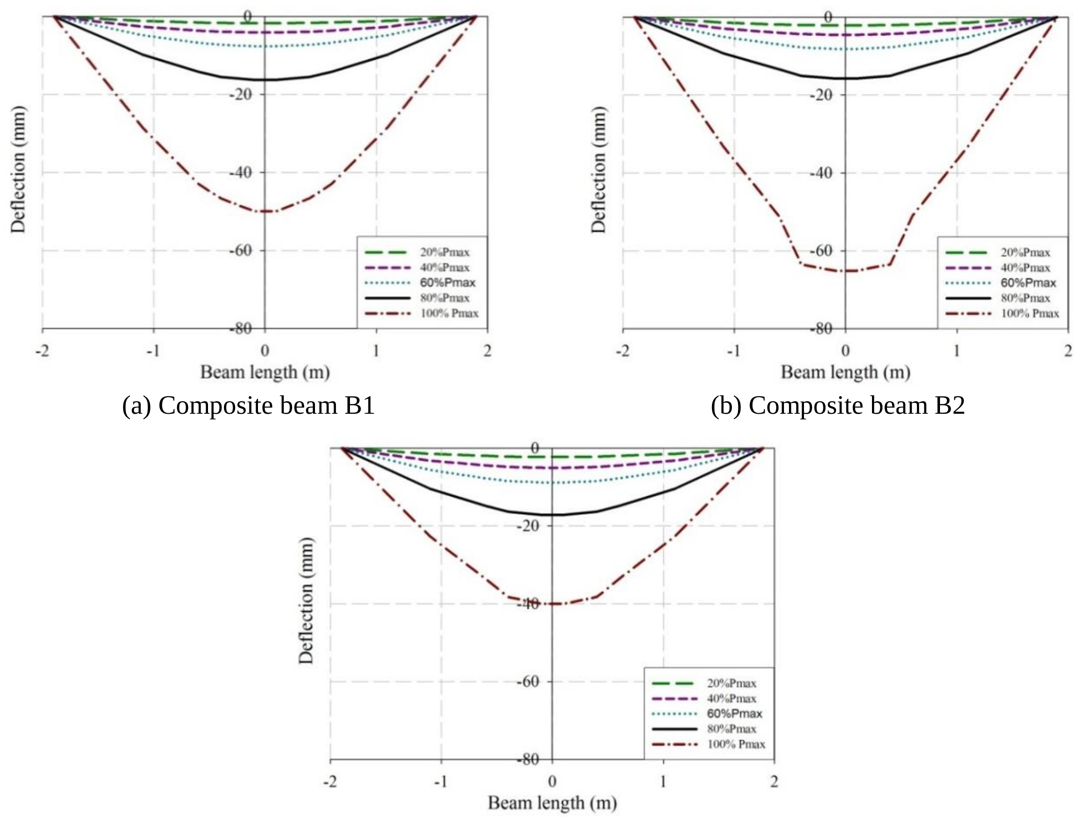

(a) Composite beam B1 (b) Composite beam B2

(c) Composite beam B3

Fig. 10 Load levels–deflection relationships

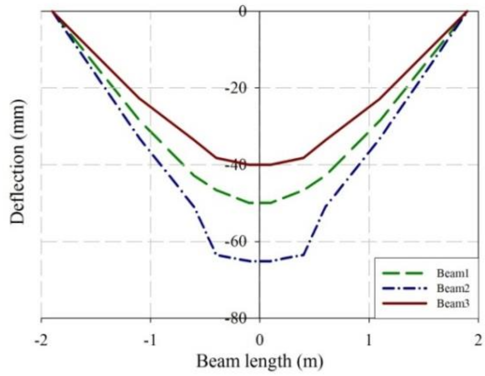

Fig. 11 Comparison of maximum load vs. deflection at mid-span curves of beams B1, B2, and B3

spans of the three beams. The deflection at the mid-span of beam B3 is the smallest, whereas that of beam B2 is the greatest. This is reasonable because the flexural stiffness of beam B3 was the highest among these beams. The ultimate load of beam B1 was 3.18% greater than that of beam B2. However, the deflection of beam B1 was 30.35% smaller than that of beam B2. This indicates that the transverse reinforcements passing through the holes did not enhance the capacity of the beams, but did beneficially affect their deflection. The concrete slab width of beam B3 was smaller than that of beam B1.

The results of a comparison of the ultimate loads and deflections at the mid-spans of beams B1 and B3 show that the ultimate load of beam B3 was 2.7% greater, whereas the deflection at the mid-span of beam B3 was 19.9% smaller. This shows that the concrete compressive strength significantly affects the behavior of concrete–steel composite beams using the newly puzzle shape of crestbond shear connectors. The ultimate load of beam B3 was slightly greater than the ultimate load of beam B1 because the dimensions of the concrete slab in beam B3 were smaller than those of beam B1, as mentioned in Table 2.

3.3 Load–relative slip at composite interface

To measure the relative slip between the concrete slab and the H beam, four LVDTs were installed at distances of 0 m, 0.3 m, 0.7 m, and 1.1 m from the end of the beam. Fig. 12 shows the load-relative slip according to the measurement position. The test results show that the relative slip is smaller at cross-sections near the support than at sections near the mid-span, as shown in Fig. 12. This is because the connection was fully shear. Therefore, the effect of the vertical shear in the support region was insignificant in comparison with that of the moment in the mid-span region.

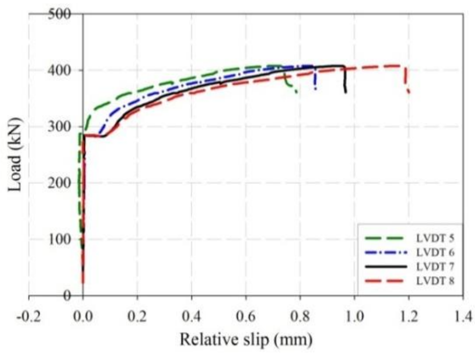

(a) Composite beam B1

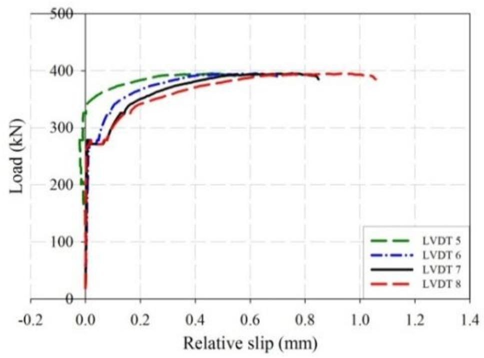

(b) Composite beam B2

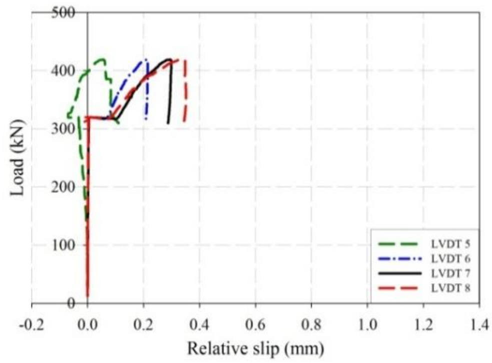

(c) Composite beam B3

Fig. 12 Load-relative slip relationships

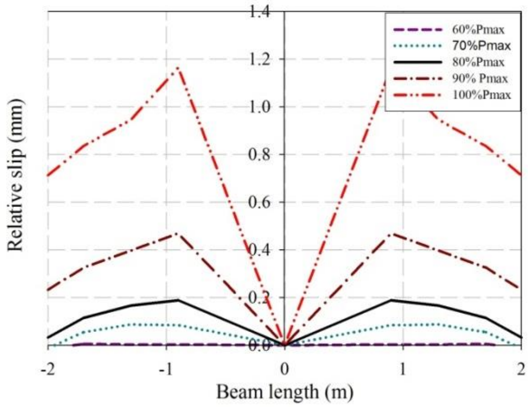

(a) Composite beam B1

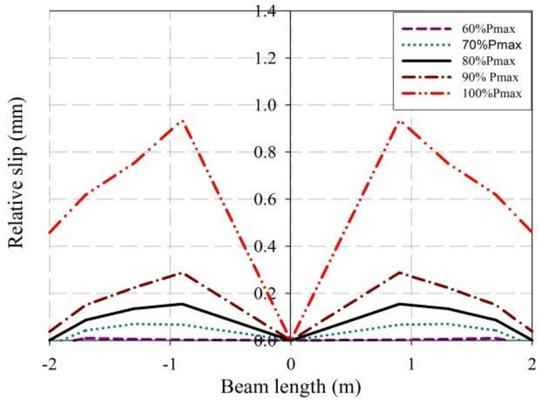

(b) Composite beam B2

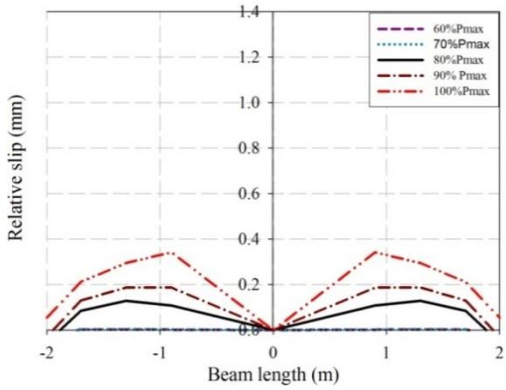

(c) Composite beam B3

Fig. 13 Load level-relative slip relationships

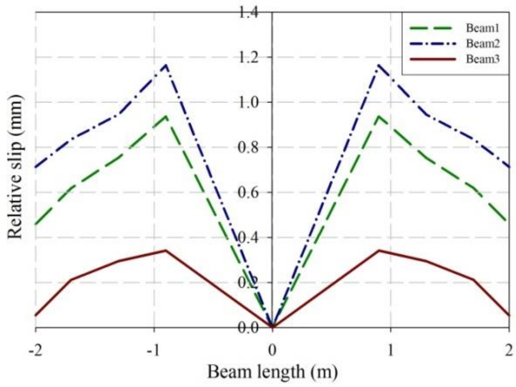

Fig. 14 Comparison of maximum load vs. relative slip at mid-span curves of beams B1, B2, and B3

Table 3 presents the relative slip recorded at LVDT8 for the ultimate load condition. At this location, the relative slip between the concrete slab and the steel girder of beam B1 was 23.4% greater than that of beam B2. This result is likely due to the different number of transverse reinforcements in the holes. In previous research, Chu, Bui *et al.* (2016), the ductility of the connectors depended on the concrete strain. Therefore, the concrete part enclosing the steel bars decreases when the transverse reinforcement is increased. Because failure of the concrete occurs more quickly, the ductility of the connectors decreases. This explains the relative results for the slip between the concrete slab and the steel beam in beams B1 and B2.

The relative slip between the concrete slab and the steel girder of beam B3 was the smallest because the stiffness of the concrete slab was greater. This delayed the failure of the concrete in the connection and resulted in increases in the ductility and shear resistance of the perfobond connector, which caused a lower relative slip between the concrete slab and the steel girder of beam B3. A comparison of the relative slips of the beams is shown in Fig. 14.

Fig. 13 shows the relative slips of the beams at various load levels. The relative slip increased significantly starting at a load of 80% P_{max}. This can be explained by the beam entering the transition from the elastic to the plastic range.

3.4 Strain of concrete slab

The strain of the concrete slab was observed by strain gauges attached at the top and bottom of the concrete slab, named SG5 and SG6. Fig. 15 shows the load-strain curves recorded at the top

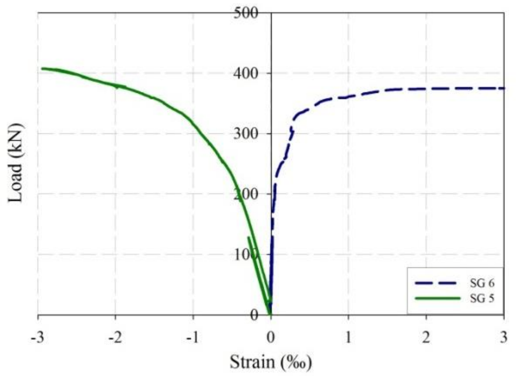

(a) Composite beam B1

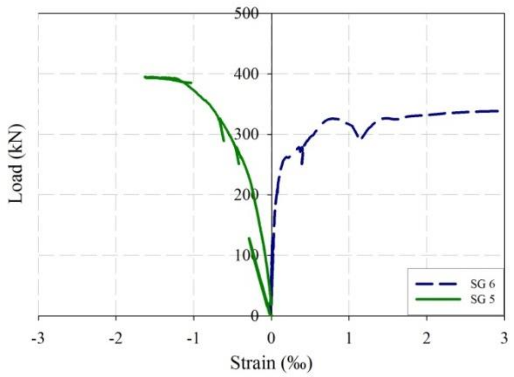

(b) Composite beam B2

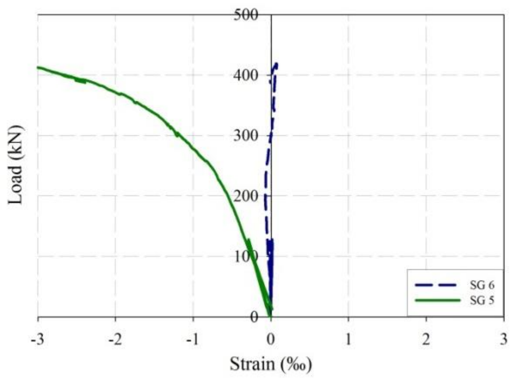

(c) Composite beam B3

Fig. 15 Load-strain relationships of concrete slabs

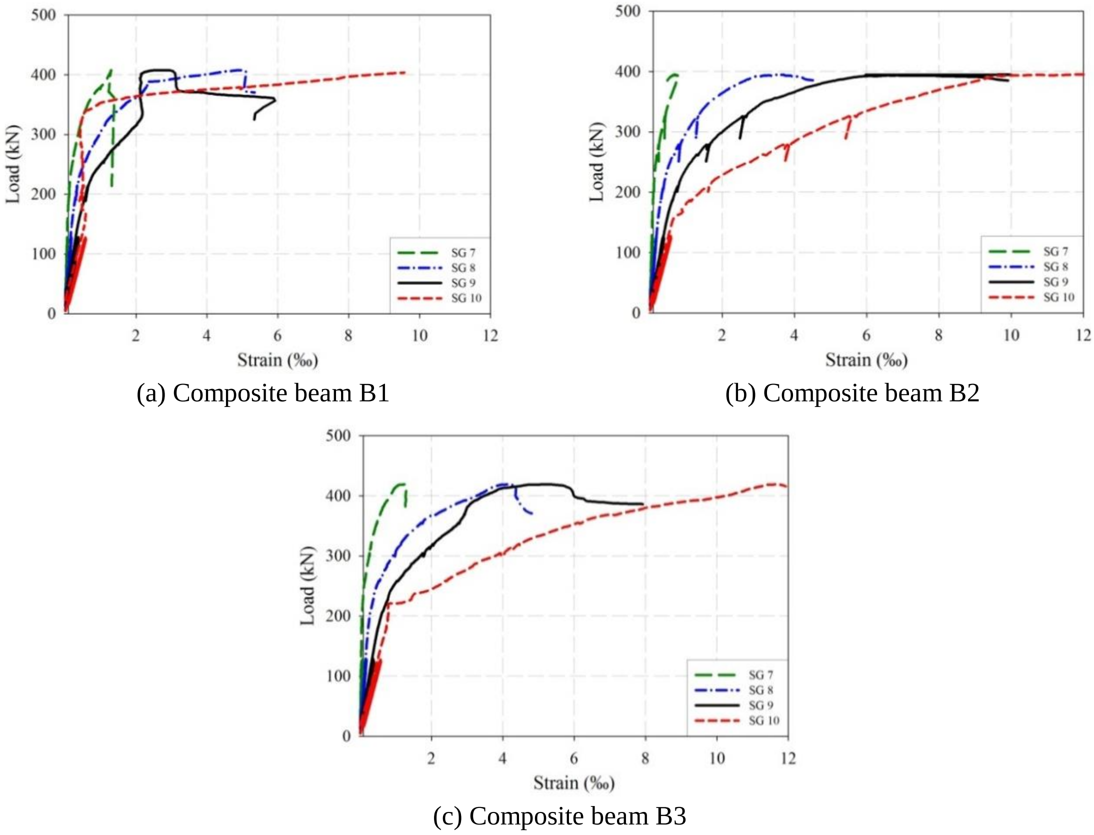

Fig. 16 Load-strain relationships of H beam

(left side) and bottom (right side) of the concrete slab. At low loading, both surfaces of the concrete slab were in compression. With increasing load, the bottom surface became gradually supported in tension. In beam B3, the compressive region lasted longer because the concrete slab of this beam was made of C40, with a compressive strength greater than that of beams B1 and B2.

3.5 Strain of H beam

The steel strain was recorded by strain gauges attached at the mid-span sections of the steel girders. Strain gauges SG7 and SG10 were attached at the top and bottom flanges of the steel girders, and SG8 and SG9 were attached at the webs of the steel girders. The strain results are shown in Fig. 16. The strain of the steel beam increases in proportion to the distance from the neutral axis to the tensile fibers. At the mid-span section, the strain of the steel girder reached the plastic yield level at the outer fiber, while the strain at the inner fibers near the centroid axis of the beam was still small at the time of beam failure.

3.6 Strain of newly puzzle shape of crestbond rib

Strain gauges SG1 to SG4 were attached to the perfobond shear connectors in order to

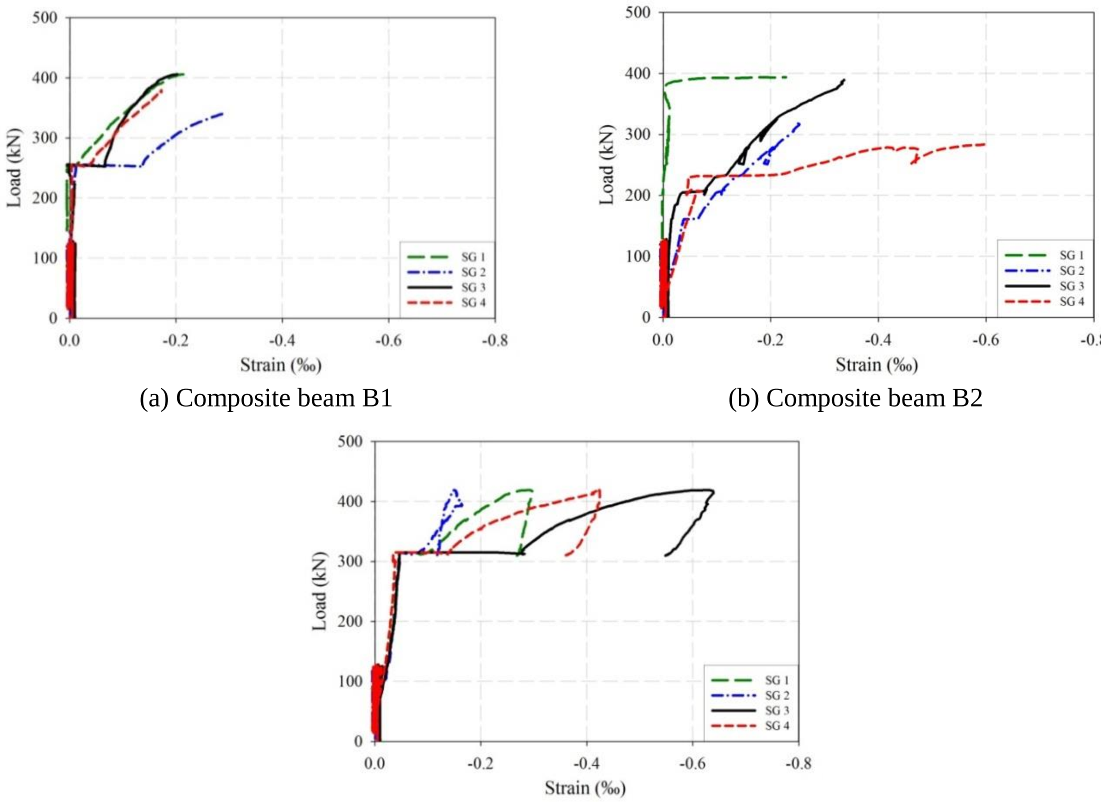

(a) Composite beam B1

(b) Composite beam B2

(c) Composite beam B3

Fig. 17 Load-strain relationships of newly revised crestbond rib.

investigate the perfobond strains at different positions. The relative slip between the steel girder and the concrete slab increased as the load increased. The perfobond strain was rather small, and the perfobond was in compression, as shown in Fig. 17. Perfobond steel has a plastic strain of 1.8‰, while the maximum measured strain was 0.65‰, which means that no failure occurred at the perfobond. Fig. 17 shows that the neutral axis (the line passing through the points where the strain equaled zero) in beam B3 is closer to the upper fiber of the steel girder than the zero lines in beams B1 and B2. This resulted in a greater compressive strain of the crestbond in beam B3 at the position where the strain gauge was attached, in comparison to those in beams B1 and B2.

3.7 Failure mode of composite beam with newly puzzle shape of crestbond rib

Failures occurred only in the concrete slab and steel girder, with no failure occurring in the perfobond shear connectors. This is entirely consistent with the strain results for the concrete slab and steel girder, as illustrated in Fig. 18, and the real conditions of the experiment failure are shown in Fig. 19. The strains in the steel girder and concrete slab exceeded 1.8‰ and 2.0‰, respectively, while the maximum perfobond strain only reached 0.65‰, as mentioned above. The results also showed that the neutral axis was lower in beam B3 than in beams B1 and B2, even though B3 was made of higher-strength concrete. This is because the concrete slab width of beam

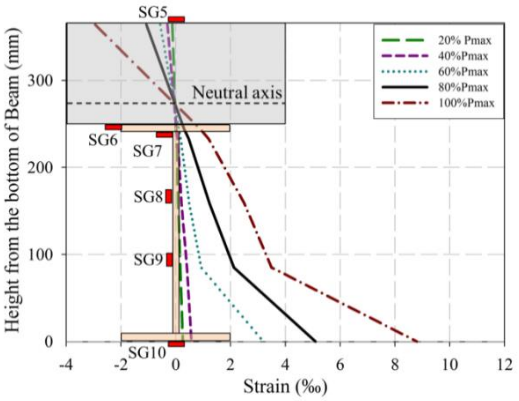

(a) Composite beam B1

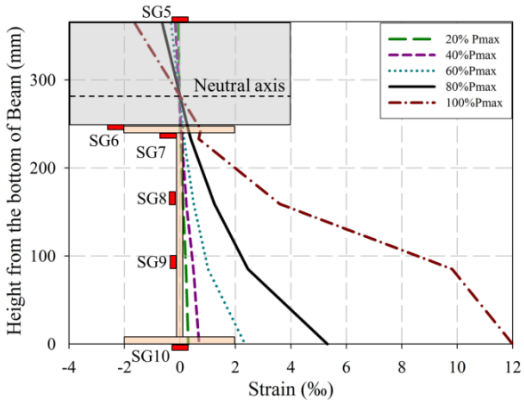

(b) Composite beam B2

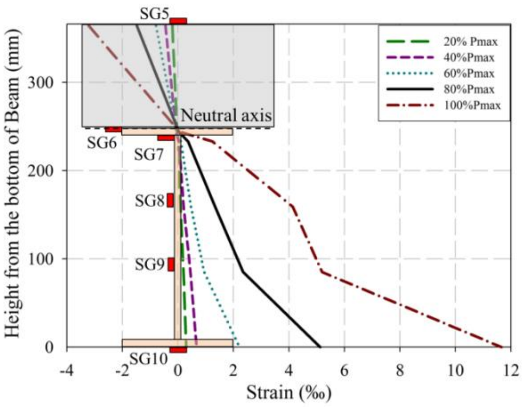

(c) Composite beam B3

Fig. 18 Failure modes of composite beam specimens.

B3 was smaller than those of beams B1 and B2, which resulted in a decrease in the hardness of the concrete slab. The neutral axis in beam B3 was very close to the upper fiber of the steel girder, whereas the zero lines in beams B1 and B2 were far from the upper fiber of the steel girder. It is assumed that the concrete compressive strength considerably affected the capacity and strain of the steel-concrete composite beams.

Fig. 18 shows that only the neutral axis of beam B3 was located correctly, based on its designation, while the neutral axes of beams B1 and B2 were located in the concrete slab. This phenomenon could have occurred because the concrete strengths of test beams B1 and B2 were higher than the designated concrete strength, and the steel plate of the crestbond helped to improve the compressive strength of the concrete slab.

4. Conclusions

In this study, static loading tests of three full-size steel–concrete composite beams with newly puzzle shape of crestbond ribs were carried out to examine the applicability of these newly puzzle

(a) Failure of concrete slab of beam B1

(b) Failure of concrete slab of beam B2

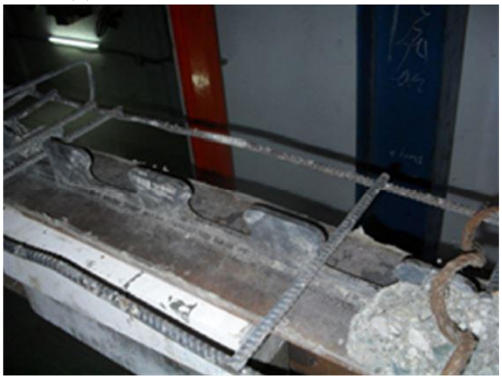

(c) Failure of steel connectors of beam B1

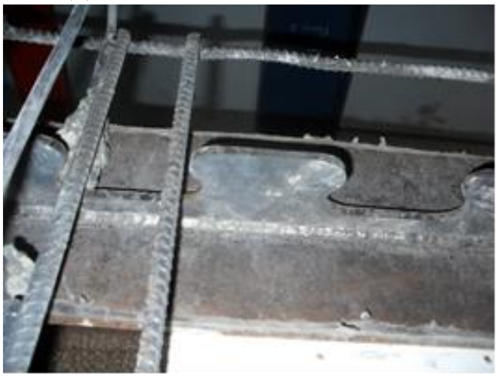

(d) Failure of steel connectors of beam B3

Fig. 19 Failure modes of composite beam specimens.

shape of crestbond ribs to composite beams, and to evaluate the effects of the transverse reinforcement and concrete compressive strength on the behaviors of composite beams with the newly puzzle shape of crestbond ribs. Therefore, the loading capacity, deflections, relative slips, strains of the crestbond ribs, and failure mechanisms of composite beams with the newly puzzle shape of crestbond ribs were quantitatively investigated. The following conclusions can be drawn:

(1) Increasing the transverse reinforcement in the concrete slab produced significantly higher ductile behaviors, as seen in push-out test results. Although the transverse rebar in a crestbond rib hole could be thought to be related to the structural characteristics, in this case the load capacity was not improved.

(2) The compressive strength of the concrete considerably influenced the behavior of the steel-concrete composite beam. Increasing the compressive strength enhanced the load capacity and decreased the deflection of the beam.

(3) The ductility of the connector depended on the concrete strain. The concrete part enclosing the steel bars decreased when the transverse reinforcement was increased, the concrete failed more quickly, and the ductility of the connector decreased.

(4) The behavior of the newly puzzle shape of crestbond in a composite beam agreed with those obtained from push-out-test specimens. Therefore, the newly puzzle shape of crestbond shear connectors could be used as shear connectors, and should be considered for application to a composite bridge, which utilizes a large number of steel beams.

Acknowledgments

This study has been supported in part by HOANG VINH Technology Research and Construction Consultants (HOANG VINH TRCC) in Vietnam. This work was also suported by the National Research Foundation of Korea (NRF) grant funded by the Korea goverment (MSIP) (No. NRF-2014R1A2A1A11054579).

References

Ahn, J.H., Lee, C.G., Won, J.H. and Kim, S.H. (2010), "Shear resistance of the perfobond rib shear connector depending on concrete strength and rib arrangement", *J. Constr. Steel Res.*, **66**(10), 1295-1307.

Bui, D.V. (2010), "Behaviour of Steel-Concrete Composite beams made of Ultra high performance concrete", *Der Wirtschaftswissenschaftlichen Fakultater Universitat Leipzig*, Leipzig, October.

Chu, T.H.V., Bui, D.V., Le, V.P.N, Kim, I.T., Anh, J.H. and Dao, D.K. (2016), "Shear resistance behaviors of a newly puzzle shape of crestbond rib shear connector: an experimental study", *Steel Compos. Struct.*, **21**(5), 1157-1182

European Committee for Standardization (Hrsg.) (2004), Eurocode 4: Design of composite steel and concrete structures, September 2004, European Committee for Standardization.

http://www.stb.rwth-aachen.de/projekte/2005/INTAB/downloadPreco.php

Kim, S.H., Ahn J.H., Choi, K.T. and Jung, C.Y. (2011), "Experimental evaluation of the shear resistance of corrugated perfobond rib shear connections", *Adv. Struct. Eng.*, **14**(2), 249-263.

Kim, S.H., Choi, J., Park, S.J., Ahn, J.H. and Jung, C.Y. (2014a), "Behavior of composite girder with Y-type perfobond rib shear connector", *J. Constr. Steel Res.*, **103**, 275-289.

Kim, S.H., Choi, K.T., Park, S.J., Park, S.M. and Jung, C.Y. (2013), "Experiment shear resistance evaluation of Y-type perfobond rib shear connector", *J. Constr. Steel Res.*, **82**, 1-18

Kim, S.H., Heo, W.H., Woo, K.S., Jung, C.Y. and Park, S.J. (2014b), "End bearing resistance of Y-type perfobond rib according to rib width-height ratio", *J. Constr. Steel Res.*, **103**, 101-116.

Kim, S.H., Kim, K.S., Park, S.J, Ahn, J.H. and Lee, M.K. (2016), "Y-type perfobond rib shear connectors subjected to fatigue loading on highway bridges", *J. Constr. Steel Res.*, **103**, 445-454.

Kim, S.H., Lee, C.G., Davaadorj, A., Yoon, J.H. and Won, J.H. (2010), "Experimental evaluation of joints consisting of parallel perfobond ribs in steel-PSC hybrid beams", *Int. J. Steel Struct.*, **10**(4), 373-384.

Kim, S.H., Park, S.J., Heo, W.H. and Jung, C.Y. (2015), "Shear resistance characteristic and ductility of Y-type perfobond rib shear connector", *Steel Compos. Struct.*, **18**(2), 497-517.

Leonhardt, F., Andrä, H.P., Harre, W. Neues. (1987), "Vorteilhaftes Verbundmittel für Stahlvebund–Tragwerke mit hoher Dauerfestigkeit", *Beton Stahlbetonbau*, **82**(12), 325-331.

Lorenc, W., Kożuch, M. and Rowiński, S. (2014), "The behaviour of puzzle-shaped composite dowels-Part I: Experimental study", *J. Constr. Steel Res.*, **101**, 482-499.

Lorenc, W., Kożuch, M. and Rowiński, S. (2014), "The behaviour of puzzle-shaped composite dowels — Part II: Theoretical investigations", *J. Constr. Steel Res.*, **101**, 500-518.

Lorenc, W., Kubica, E. and KoŻUch, M. (2010), "Testing procedures in evaluation of resistance of innovative shear connection with composite dowels", *Arch. Civil Mech. Eng.*, **10**, 51-63.

Mohammad, M.A., Ayad, S.A. and Bilavari, K. (2011), "Performance evaluation of shear stud connectors in composite beams with steel plate and RCC slab", *Int. J. Earth Sci. Eng.*, **4**(6), 586-591

PreCo-Beam (2009), Prefabricated enduring composite beams based on innovative shear transmission, Final Report, Research Fund for Coal and Steel, Contract No. RFSR-CT-2006-00030. 01/07/2006-30/06/2009.

Preco+ (2016), Prefabricated Enduring Composite Beams based on innovative Shear Transmission; RFCS RFS2-CT-2011-00026, Research Fund for Coal and Steel (RFCS) of the European Community, EU, http://www.stb.rwth-aachen.de/projekte/2005/INTAB/downloadPreco.php

Rovnak, M., Duricova, A. and Ivanco, V. (2000), "Non-traditional shear connections in steel-concrete composite structures", *Proc. 6th ASCCS Conf. on Steel and Concrete Composite Structures*, Los Angeles, 305-312.

Shariati, M., Ramli, N.H., Arabnejad, M.M. Sulong, K.H. and Mahoutian, M. (2011), "Shear resistance of channel shear connectors in plain,reinforced and lightweight concrete", *Sci. Res. Essay.*, **6**(4), 977-983.

Shim, C.S., Lee, P.G., Kim, D.W. and Chung, C.H. (2011), "Effects of Group Arrangement on the Ultimate Strength of Stud Shear Connection", *Compos. Constr. Steel Concrete*, **6**, 92-101.

Xue, D., Liu, Y., Yu, Z. and He, J. (2012), "Static behavior of multi-stud shear connectors for steel-concrete composite bridge", *J. Constr. Steel Res.*, **74**, 1-7.

CC